

# Mutagenesis of the Ezrin-Radixin-Moesin Binding Domain of L-selectin Tail Affects Shedding, Microvillar Positioning, and Leukocyte Tethering\*

Received for publication, November 7, 2003, and in revised form, June 2, 2004  
Published, JBC Papers in Press, June 3, 2004, DOI 10.1074/jbc.M312212200

Aleksandar Ivetić<sup>‡§</sup>, Oliver Florey<sup>¶</sup>, Jürgen Deka<sup>||\*\*</sup>, Dorian O. Haskard<sup>¶</sup>, Ann Ager<sup>‡‡</sup>,  
and Anne J. Ridley<sup>‡§§</sup>

From the <sup>‡</sup>Ludwig Institute for Cancer Research, Royal Free and University College School of Medicine, 91 Riding House Street, London W1W 7BS United Kingdom, <sup>¶</sup>BHF Cardiovascular Medicine Unit, Imperial College, Hammersmith Hospital, Du Cane Road, London W12 0NN, United Kingdom, the Divisions of <sup>||</sup>Protein Structure and <sup>‡‡</sup>Immune Cell Biology, The National Institute for Medical Research, London NW7 1AA, United Kingdom, and the <sup>§§</sup>Department of Biochemistry and Molecular Biology, University College, London WC1E 6BT, United Kingdom

**L-selectin is a cell adhesion molecule that mediates the initial capture (tethering) and subsequent rolling of leukocytes along ligands expressed on endothelial cells. We have previously identified ezrin and moesin as novel binding partners of the 17-amino acid L-selectin tail, but the biological role of this interaction is not known. Here we identify two basic amino acid residues within the L-selectin tail that are required for binding to ezrin-radixin-moesin (ERM) proteins: arginine 357 and lysine 362. L-selectin mutants defective for ERM binding show reduced localization to microvilli and decreased phorbol 12-myristate 13-acetate-induced shedding of the L-selectin ectodomain. Cells expressing these L-selectin mutants have reduced tethering to the L-selectin ligand P-selectin glycoprotein ligand-1, but rolling velocity on P-selectin glycoprotein ligand-1 is not affected. These results suggest that ERM proteins are required for microvillar positioning of L-selectin and that this is important both for leukocyte tethering and L-selectin shedding.**

L-selectin mediates tethering and subsequent rolling of leukocytes on endothelial cells. Leukocytes derived from L-selectin-null mice home poorly to lymph nodes and sites of inflammation, indicating an essential role for L-selectin in initiating leukocyte transendothelial migration (1, 2). L-selectin ligands such as glycosylation-dependent cell adhesion molecule-1 or P-selectin glycoprotein ligand-1 (PSGL-1)<sup>1</sup> support tethering and rolling of leukocytes on endothelial cells and other leukocytes, respectively (3). Upon leukocyte activation (e.g. by phorbol 12-myristate 13-acetate (PMA), inter-

leukin-8, T-cell receptor stimulation, or lipopolysaccharide stimulation (4, 5)), L-selectin is rapidly proteolyzed at a specific extracellular site proximal to the plasma membrane, leading to shedding of the ectodomain from the cell surface (6, 7). Several reports have implicated the protease A disintegrin and metalloproteinase 17 (ADAM17) in mediating PMA-induced shedding of L-selectin (8–10).

The 17-amino acid-long cytoplasmic tail of L-selectin can bind to several proteins that are implicated in regulating its function. In resting cells, the membrane-proximal region of the L-selectin tail interacts with calmodulin (11, 12). Upon PMA stimulation, calmodulin is released from the L-selectin tail, and this is predicted to induce a conformational change in the ectodomain that may render the L-selectin cleavage site susceptible to proteolysis. Calmodulin antagonists can also induce rapid shedding of L-selectin in the absence of PMA stimulation, suggesting that calmodulin negatively regulates L-selectin shedding. However, such antagonists have been shown to induce shedding of other integral membrane proteins, suggesting that this mechanism is not specific for L-selectin (13). The membrane-distal portion of L-selectin tail is reported to interact with the cytoskeletal protein  $\alpha$ -actinin (14). Cells expressing L-selectin with a deletion of the  $\alpha$ -actinin binding domain (known as L $\Delta$ cyto) were initially shown to bind L-selectin ligand but failed to roll *in vivo* (15), suggesting that  $\alpha$ -actinin was important for rolling. Transmission electron microscopy revealed that L $\Delta$ cyto, like wild type L-selectin, is localized to the tips of microvilli (14). More recently, *in vitro* microkinetic analysis of cells expressing L $\Delta$ cyto demonstrated that they are in fact able to tether and roll, although less efficiently than cells expressing wild type L-selectin (16). This suggests that the six-amino acid-long tail of L $\Delta$ cyto contributes to microvillar positioning and is sufficient to mediate tethering and rolling.

We have recently shown that two members of the ezrin-radixin-moesin (ERM) family of proteins, ezrin and moesin, can bind to the L-selectin tail (17). ERM proteins are involved in the formation of membrane/actin cytoskeletal structures (18), such as membrane ruffles, microvilli (19), and cleavage furrows (20, 21). They link integral membrane proteins, such as CD44 (22), intercellular adhesion molecules 1, 2, and 3 (23–26), CD43 (20, 27), PSGL-1 (28, 29), and CD31 (30), with the cortical actin cytoskeleton. ERM-binding sites on the cytoplasmic tails of these proteins are often close to the membrane and contain basic amino acid residues.

Using a biochemical screen, we have determined the relative contribution of different basic amino acids within the L-selectin

\* This work was supported by the Ludwig Institute for Cancer Research and European Community Contract QLGI-CT-99-013036 (to A. A. and A. J. R.), the Medical Research Council (United Kingdom) (to A. A.), the British Heart Foundation (to O. F. and D. O. H.), and an EU Marie Curie Fellowship (to J. D.). The costs of publication of this article were defrayed in part by the payment of page charges. This article must therefore be hereby marked "advertisement" in accordance with 18 U.S.C. Section 1734 solely to indicate this fact.

§ To whom correspondence should be addressed. Tel.: 44-20-7878-4036; Fax: 44-20-7878-4040; E-mail: aleks@ludwig.ucl.ac.uk.

\*\* Present address: ISREC, Chemin des Boveresses 155, 1066 Epalinges s/Lausanne, Switzerland.

<sup>1</sup> The abbreviations used are: PSGL-1, P-selectin glycoprotein ligand-1; PMA, phorbol 12-myristate 13-acetate; ADAM17, A disintegrin and metalloproteinase 17; ERM, ezrin-radixin-moesin; FITC, fluorescein isothiocyanate; FACS, fluorescence-activated cell sorting; PBS, phosphate-buffered saline; BSA, bovine serum albumin; rPSGL, recombinant P-selectin glycoprotein ligand-1; WT, wild type.

tail on binding to the N-terminal domain of moesin. Two amino acid residues, Arg<sup>357</sup> and Lys<sup>362</sup>, were found to be most critical for moesin binding. Using murine 300.19 pre-B cells, stable transfectants expressing wild type L-selectin or L-selectin with alanine mutations at position Arg<sup>357</sup> or Lys<sup>362</sup> (termed R357A and K362A, respectively) were generated to address the role of ERM binding on L-selectin function. The ERM-binding mutants of L-selectin exhibited defects in PMA-induced shedding, microvillar positioning, and tethering, indicating that ERM proteins play a key role in L-selectin function.

#### EXPERIMENTAL PROCEDURES

**Materials**—Unless otherwise stated, all chemicals were purchased from Sigma. Murine anti-human L-selectin monoclonal antibodies DREG200 (Santa Cruz Biotechnology, Inc., Santa Cruz, CA) and FMC46 FITC-conjugated anti-L-selectin (DAKO) were used for immunogold labeling and fluorescence-activated cell sorting (FACS) analysis, respectively. CA21 mouse monoclonal and JK924 rabbit polyclonal (kindly provided by Julius Kahn; Roche Applied Science) antibodies recognize the membrane-distal portion of the L-selectin tail and the membrane-proximal ectodomain of L-selectin, respectively (11). Goat anti-mouse antibody conjugated to 20-nm colloidal gold particles (BBInternational) was used as a secondary antibody for immunogold labeling of L-selectin. Affinity-purified mouse anti-calmodulin antibody was a kind gift from David Sacks (Harvard Medical School) and was used at a dilution of 1:3000 for immunoblotting. Sheep anti-mouse F(ab')<sub>2</sub> conjugated to horseradish peroxidase (Amersham Biosciences) was used as a secondary antibody for immunoblotting at a dilution of 1:3000. FITC-conjugated KPL1 (Santa Cruz Biotechnology) was used to detect immobilized rPSGL-1-Ig.

**Cells**—300.19 pre-B cells were kindly provided by Thomas Tedder (Duke University). Cells were maintained at 37 °C in 5% CO<sub>2</sub> under humidifying conditions. Cells were cultured in RPMI 1640 containing L-glutamine (Invitrogen), 10% fetal calf serum (Helena Biosciences), 1% (v/v) of 100 units/ml penicillin and streptomycin (Invitrogen), 50 μM β-mercaptoethanol, and, under selection conditions, 2 μg/ml puromycin. Cells were grown at densities no greater than 2.5 × 10<sup>6</sup>/ml.

**Mutagenesis of Human L-selectin Tail**—pMT2 plasmid containing the cDNA of WT L-selectin (LAM/pMT2) was a kind gift from Thomas Tedder and was used as the template for generating the two ERM-binding mutants. QuikChange<sup>TM</sup> (Stratagene) PCR mutagenesis was performed according to the manufacturer's instructions to generate R357A and K362A mutants. The open reading frames of both mutants were sequenced to ensure that only the correct mutations had been incorporated. The primers (all written in the direction of 5' to 3') used for mutagenesis were as follows: R357A forward, CTCATTTGGCTGGCAAGGGCGTTAAAAAAGGCAGAAATCTC; R357A reverse, GAG-ATTTCTTCCCTTTTTTAACGCCCTTGCCAGCCAAATGAG; K362A forward, GGCGGTTAAAAAAGCGCGGAAATCTCAAGAAAGGATGG; K362A reverse, CCATCCTTCTTGAGATTCGCGCCTTTTTTTAACC GCC.

**Generation of Stable Transfectants**—300.19 cells were grown overnight at a starting density of 1 × 10<sup>6</sup>/ml. The following day, for each transfection, 1 × 10<sup>7</sup> cells were harvested and washed twice in serum-free RPMI 1640 followed by resuspension in 300 μl of electroporation buffer (120 mM KCl, 2 mM MgCl<sub>2</sub>, 10 mM K<sub>2</sub>PO<sub>4</sub>/KH<sub>2</sub>PO<sub>4</sub>, pH 7.6, 0.5% Ficoll 400, 25 mM HEPES, pH 7.6). For each electroporation, 20 μg of pMT2 plasmid containing the open reading frame of L-selectin (WT or mutants) was mixed with 2 μg of pBabe plasmid containing the puromycin resistance gene. Cells were transferred to a precooled 0.4-cm electroporation cuvette (Bio-Rad), electroporated at 1180 microfarads and 400 mV in a Bio-Rad Gene Pulser and placed immediately on ice for 5 min. Cells were subsequently transferred to standard growth medium and were left to recover for 2 days. Transfected cells were subsequently selected in growth medium containing puromycin (2 μg/ml).

Cells were labeled using FITC-conjugated L-selectin (DAKO) at a dilution of 1:500 and subsequently sorted using a FACScan (Beckman-Coulter EPICS Elite flow cytometer) under sterile conditions. Pooled clones were gated to achieve similar levels of L-selectin expression. Sorted cells were subsequently seeded and cultured in 6-well dishes.

All cells were propagated and subsequently frozen in liquid nitrogen for long term storage. Cells were maintained in culture for ~6 weeks without any loss of L-selectin expression. Cells were analyzed by flow cytometry prior to each experiment to ensure that levels of L-selectin were consistent.

**Immunoprecipitation and Immunoblotting**—For each immunopre-

cipitation, 1 × 10<sup>7</sup> cells were harvested and lysed using lysis buffer (1% Triton X-100, 25 mM Tris-HCl (pH 7.4), 150 mM NaCl, EDTA-free protease inhibitor mixture (Roche Applied Science)). Lysis buffer was used for washing immunoprecipitates. After a 15-min incubation on ice, cells were centrifuged at 13,000 × g, and supernatants were retained for immunoprecipitation. Lysates were precleared for 2 h with protein A-Sepharose beads prior to incubation with 5–10 μl of antiserum JK294. After 2 h, 10 μl of protein A-Sepharose beads (slurry) was added to the antibody/lysate mixture for 1 h. At least four (1-ml) washes were performed for each immunoprecipitate. Immunoprecipitates were separated by SDS-PAGE and immunoblotting as described before (17).

**BIAcore-based Competition Assay**—The pQE expression vector encoding the N-terminal domain of human moesin (residues 1–296) was a kind gift from Anthony Bretscher (Cornell University). N-terminal moesin was expressed in *Escherichia coli* and purified according to a previously published protocol (31). Surface plasmon resonance was performed using a BIAcore system (BIAcore AB, Uppsala, Sweden). The general principles of this method were reviewed recently (32). To avoid covalent inactivation of essential side chains, the entire cytoplasmic tail of L-selectin was synthesized as a biotinylated peptide (conjugated to Arg<sup>356</sup>) and immobilized on the sensor surface using a noncovalent sandwich system. The peptide was coupled via the N-terminal biotin moiety to a streptavidin-coated sensor chip (BIAcore AB).

For analyzing interactions between N-terminal moesin and immobilized L-selectin peptide, 5 μM purified N-terminal moesin was injected in 10 mM HEPES (pH 7.4), 150 mM NaCl, 0.005% (v/v) polysorbate 20 (HSP-P; BIAcore AB) with a flow rate of 5 μl/min. A short wash in the same buffer removed excess, unbound N-terminal moesin from the L-selectin tail. Peptides used in competition assays were injected at a concentration of 100 μM over a period of ~400 s. Regeneration of the sensor surface was achieved by injection of 100 mM NaOH followed by subsequent reloading of the sensor surface with 1 μM biotinylated L-selectin cytoplasmic tail. All measurements were monitored at 25 °C.

**Solid Phase Binding Assays**—N-terminal moesin was immobilized onto microtiter wells for 1 h at room temperature or overnight at 4 °C. Wells were subsequently washed with PBS and blocked for 1 h in PBS containing 1% BSA. Biotinylated peptides were prepared in PBS containing 1% BSA at a concentration of 1 μM and subsequently added to the appropriate wells for 1 h at room temperature. Wells were subsequently washed three times in PBS. Streptavidin-horseradish peroxidase was prepared in PBS containing 1% BSA and added to wells for 1 h at room temperature. Wells were washed a further three times in PBS prior to color development, using TMB peroxidase EIA substrate kit (Bio-Rad). All absorbance readings were monitored at a wavelength of 450 nm, and values were subtracted against peptides bound to BSA-coated wells (*i.e.* in the absence of N-terminal moesin).

**Immunogold Labeling of Stable Transfectants and Transmission Electron Microscopy**—Stable transfectants were harvested and resuspended at a density of 1 × 10<sup>6</sup>/ml. Cells were labeled on ice for 30 min with 10 μg/ml DREG 200 monoclonal antibody in RPMI 1640 containing 1% BSA. After washing excess primary antibody, cells were labeled on ice for 30 min with secondary 20-nm colloidal gold-conjugated secondary antibody (1:10). Cells were washed twice in PBS and subsequently fixed for 15 min at room temperature with a mixture of 4% paraformaldehyde and 0.1% glutaraldehyde. After washing cells twice with 1% BSA, to block any reactivity of the fixation solution, cells were harvested into pellets and were kept warm at 40 °C. Pellets were resuspended in molten low melting point agarose and then immediately placed on ice. Once set, the agarose block was cut into 1-mm<sup>3</sup> pieces for further treatment. Sectioning and mounting was undertaken by Dr. Mark Turmaine (Anatomy Department, University College London). All sections were examined using a Jeol 1010 transmission electron microscope. Gold particles were scored according to positioning on distinct membrane structures (cell body or microvilli). All experiments were performed in triplicate and assessed single blind. Approximately 35 cells were analyzed for each individual cell line. Minimal labeling of L-selectin-negative puromycin-resistant 300.19 cells was observed (data not shown).

**Parallel Plate Flow Assay**—Nunc Slide Flaskettes (9 cm<sup>2</sup>; Nalge Nunc International) were disassembled in order to use the slide for rolling assays. Recombinant P-selectin glycoprotein ligand-1 fused to human heavy chain immunoglobulin (rPSGL-1-Ig; a kind gift from Wyeth Research, Cambridge, MA) was spotted (50 μl) onto plastic slides at the indicated concentrations and incubated overnight under humidifying conditions at 4 °C. Excess rPSGL-1-Ig was removed the next day by gentle washing with PBS, after which slides were immersed in PBS containing 1% BSA for 2 h at room temperature. Slides were washed twice with PBS, 0.05% Tween 20 prior to use and mounted in a parallel

TABLE I

Panel of synthetic peptides used to screen for interaction of N-terminal moesin with L-selectin tail

The position of each alanine is underlined and indicated in boldface type. Y327A was used as a control peptide that carried an alanine mutation but not in the position of a basic residue.

Peptide name	Sequence	Modification
R356A	ARLKKGKKSKRSMNDPY	
R357A	RALKKGKKSKRSMNDPY	
K359A	RRLAKGKKSKRSMNDPY	
K360A	RRLKAGKKSKRSMNDPY	
K362A	RRLKKGAKSKRSMNDPY	
K363A	RRLKKGKASKRSMNDPY	
K365A	RRLKKGKKSARSMNDPY	
Y372A	RRLKKGKKSKRSMNDPA	
WT	RRLKKGKKSKRSMNDPY	
Scram	PRSYKSRKGNLKRKDKM	
Bio-WT	RRLKKGKKSKRSMNDPY	N-terminal biotinylation
Bio-R357A	RALKKGKKSKRSMNDPY	N-terminal biotinylation
Bio-K362A	RRLKKGAKSKRSMNDPY	N-terminal biotinylation

plate flow chamber (channel height 0.15 cm). Stable transfectants expressing WT or mutant L-selectin were resuspended at a density of  $3 \times 10^6$ /ml in Hanks' balanced salt solution (Invitrogen) and 2% BSA (viscosity 0.007 poise) and perfused at 37 °C over rPSGL-1-Ig-coated slides at a fixed shear stress of 2.5 dynes/cm<sup>2</sup>. Experiments were visualized using a Diaphot 300 inverted fluorescence microscope (Nikon) connected to a JVC TK-C1360B color video camera and recorded on a Panasonic AG-6730 S-VHS video recorder (Microscope Service and Sales). 10 random fields were recorded for 15 s each using a  $\times 10$  objective (800  $\times$  600 mm<sup>2</sup>). Images were acquired into a video file (In Video PCI; Focus Enhancements, Campbell, CA) at 15 frames/s, and numbers of cells undergoing rolling and/or arrest, rolling velocity of individual cells, and mean velocity of the population were calculated using EML Motion Analysis software (Ed Marcus Laboratories, Boston, MA). Rolling cells were defined as those with a mean velocity from 3  $\mu$ m/s to 200  $\mu$ m/s for at least 1 s; adherent cells were specified as those moving less than 3  $\mu$ m in 10 s. Mean rolling velocity was calculated from measurements of at least 300 cells in each independent experiment.

**Determination of Saturating Levels of rPSGL-1-Ig**—Black polystyrene 96-well plates (Nunc) were used to analyze saturating levels of rPSGL-1-Ig. The binding method followed the same format as that described for immobilizing N-terminal moesin (see above). rPSGL-1-Ig was similarly blocked in PBS containing 1% BSA. FITC conjugate KPL1 antibody was used to detect immobilized PSGL-1 at a dilution of 1:100. Plates were read using a Fusion  $\alpha$ -FP™ fluorimeter (PerkinElmer Life Sciences), and excitation and emission wavelengths were set at 485 and 535 nm, respectively.

**Tethering Analysis**—Analyses of transient tethering events were performed on slides coated with rPSGL-1-Ig at 31.7  $\mu$ g/ml. Cells at a density of  $3 \times 10^6$ /ml were perfused at 2.5 dynes/cm<sup>2</sup>. Transient tethering interactions, which were observed in cell trajectory reconstructions as a clear pause from free flow, were defined as episodes where cells achieved a minimum velocity below the threshold for rolling, 200  $\mu$ m/s for between 0.2 and 1 s. Results are expressed as the number of tethering events/min.

## RESULTS

**Identification of Amino Acid Residues within the L-selectin Tail That Are Important for Interaction with Moesin**—Membrane-proximal basic amino acid residues within the cytoplasmic tails of several cell adhesion molecules are required for binding to the N-terminal domain of ERM proteins (25). BIAcore affinity analysis was employed to determine the relative contribution of each basic amino acid within the L-selectin tail upon binding to the N-terminal domain of moesin. As previously described, a synthetic biotinylated peptide encoding the L-selectin tail (see Table I) was immobilized on a streptavidin-coated sensor chip and used as a ligand for N-terminal moesin. N-terminal moesin was injected into the sensor chip to allow it to bind to L-selectin tail. After a short wash (to remove any excess unbound N-terminal moesin), 100  $\mu$ M competitor peptide containing the entire sequence of L-selectin tail was injected.

Injection of peptides at or exceeding concentrations of 500  $\mu$ M led to nonspecific competition. Peptide concentrations below 100  $\mu$ M were found not to compete (data not shown). Injection of wild type (WT) peptide induced release of N-terminal moesin from the biotinylated WT L-selectin tail on the chip (Fig. 1A), indicating that it competed effectively for binding to N-terminal moesin.

A panel of synthetic competitor peptides (see Table I), each containing a single alanine mutation in place of a basic amino acid residue, was used to address which amino acids were required to compete N-terminal moesin from the WT L-selectin tail. Alanine-substituted residues in peptides that failed to compete N-terminal moesin from the L-selectin tail were considered necessary for interaction with ERM proteins. In contrast, alanine-substituted residues in peptides that could successfully compete N-terminal moesin from the L-selectin tail were considered unnecessary for interaction with ERM proteins. None of the competitor peptides could compete as well as WT, indicating that all 8 basic residues in the L-selectin tail contribute to ERM binding. However, the peptides fell into three groups based on their ability to compete: those that could not compete at all (Fig. 1B), those that competed only mildly (Fig. 1C), and those that competed best (Fig. 1D). The sensorgram profiles of K362A and R357A were similar to the profile of scrambled peptide (compare sensorgrams in Fig. 1, A and B), indicating that these particular peptides had the weakest ability to compete with WT L-selectin. Interestingly, although only one amino acid residue apart, R356A competed for binding to N-terminal moesin significantly better than R357A (compare profile of R357A in Fig. 1B with profile of R356A in Fig. 1D).

Solid phase binding assays were performed to further substantiate the relative binding capacities of WT, R357A, and K362A peptides to N-terminal moesin. A range of concentrations of N-terminal moesin were immobilized onto microtiter wells (see "Experimental Procedures") and subsequently incubated with 1  $\mu$ M biotinylated WT, R357A, or K362A peptide. Unlike WT peptide, both R357A and K362A peptides did not bind detectably to N-terminal moesin across a range of dilutions (Fig. 1E).

These results indicate that Arg<sup>357</sup> and Lys<sup>362</sup> of L-selectin tail are necessary for interaction with N-terminal moesin. We previously reported that Arg<sup>357</sup> was important for binding to ERM proteins (17), and the present results show that this amino acid together with Lys<sup>362</sup> are the most important for moesin binding of the 8 basic amino acids in the L-selectin tail.

**Generation of Stable Transfectants Expressing WT, R357A, and K362A L-selectin**—The 300.19 pre-B-cell line has previously been used to study L-selectin biology (33–35). In order to study the role of L-selectin/ERM interaction in cells, we generated 300.19 pre-B cell lines expressing WT, R357A, and K362A human L-selectin. L-selectin-positive cells were selected by flow cytometry (Fig. 2). The K362A cell line contained a subpopulation of cells with lower L-selectin levels (see below).

**ERM-binding mutants of L-selectin Co-immunoprecipitate Calmodulin**—Several reports indicate that L-selectin shedding is regulated by the calcium-binding protein, calmodulin (11, 12). The mutations R357A and K362A are located close to where calmodulin has been reported to bind. To address whether these mutations affect binding to calmodulin, L-selectin was immunoprecipitated with the antiserum JK924, which recognizes the extracellular membrane-proximal domain of human L-selectin. Immunoblot analysis revealed that calmodulin co-precipitated with WT, R357A, and K362A L-selectin (Fig. 3). Although one of the alanine mutations, R357A, is juxtaposed to an amino acid residue that is required for calmodulin binding (leucine 358), this mutation appeared not to affect interaction

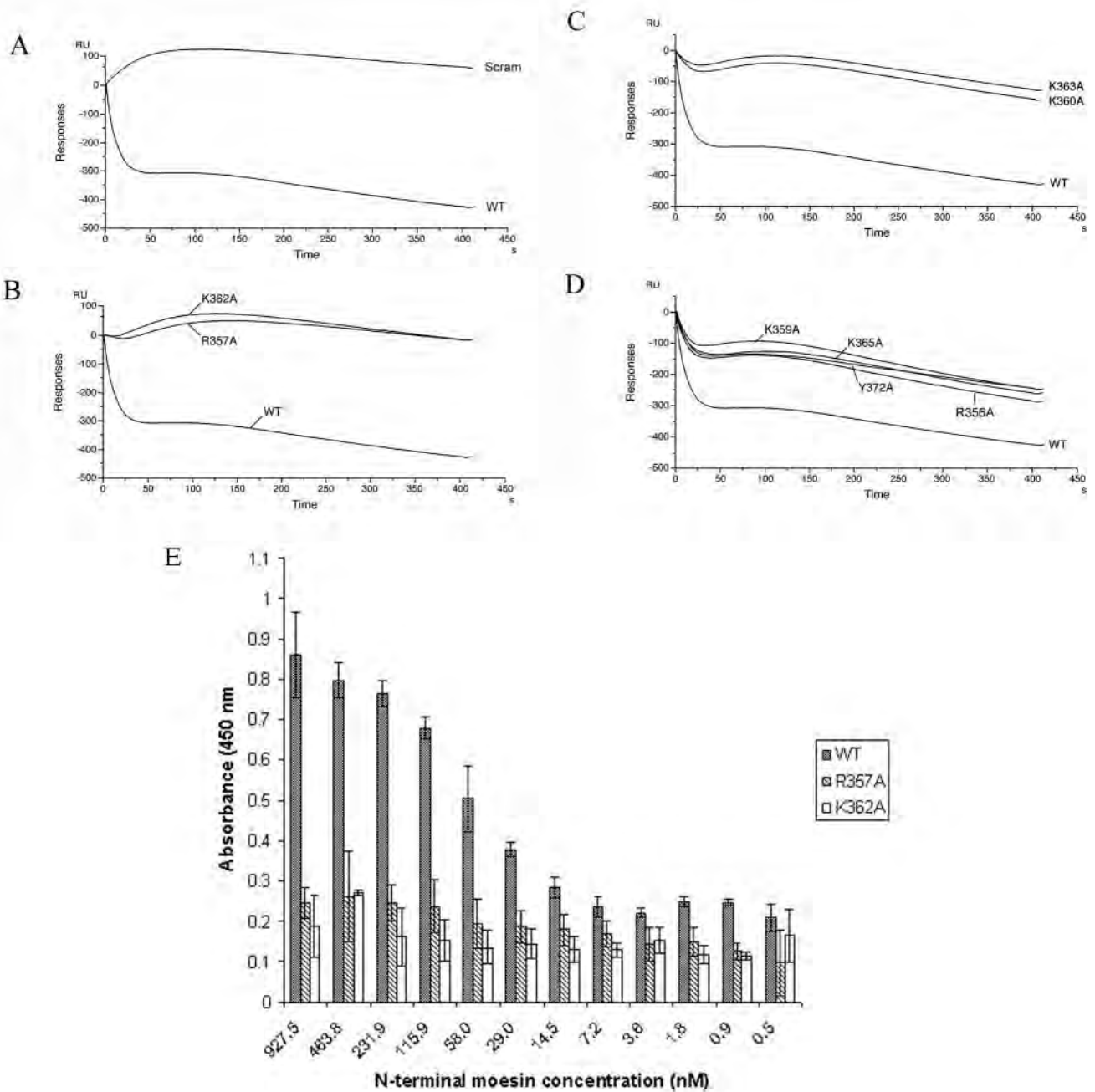


**FIG. 1. Moesin binding to L-selectin tail mutants.** Biotinylated WT L-selectin peptide was immobilized on to the sensor chip as detailed under “Experimental Procedures.” Sensorgrams depict readings taken from the point of injection of competitor peptide. Peptides were categorized into three groups: those that could not compete at all with the immobilized WT L-selectin peptide (*B*), those that competed mildly (*C*), and those that competed best (*D*). For comparison, competition using WT L-selectin tail is shown in each *panel*. The sensorgram in *A* compares maximal and minimal peptide competition using WT and scrambled (*Scram*) peptides, respectively. *E*, solid phase binding assay, determining the relative binding capacities of WT, R357A, and K362A peptides to serial doubling dilutions of N-terminal moesin coated on microtiter wells. Results represent mean  $\pm$  S.D. of three independent experiments.

with calmodulin. These results suggest that the mutations engineered in the L-selectin tail specifically affect ERM protein binding and do not abrogate interaction with calmodulin.

*The ERM-binding Mutants R357A and K362A Show Reduced PMA-induced Shedding*—PMA-induced shedding of L-selectin is rapid and occurs within minutes (4, 7, 36–39). Stimulation of 300.19 cells expressing L-selectin with  $1 \mu\text{M}$  PMA for 15 min resulted in loss of L-selectin from cells expressing WT and K362A L-selectin (Fig. 4A), but cells expressing R357A L-selectin appeared to resist PMA-induced shedding (Fig. 4A).

Further detailed analysis, using a range of PMA concentrations, revealed that shedding of K362A L-selectin was also lower

than WT L-selectin. At 10 nM PMA, cells expressing WT L-selectin had shed over 60% of surface L-selectin, leaving  $\sim$ 40% still associated with the cell surface (Fig. 4B). In contrast, at the same concentration of PMA, cells expressing R357A and K362A L-selectin resisted shedding, retaining surface levels of  $\sim$ 80 and 60%, respectively. These results clearly demonstrate that both R357A and K362A L-selectin are able to resist PMA-induced shedding at low concentrations of PMA. At higher concentrations of PMA, however, only cells expressing R357A L-selectin were able to resist shedding to a significant degree.

*R357A and K362A L-selectin Show Reduced Localization to Microvilli*—L-selectin is normally clustered on microvilli of

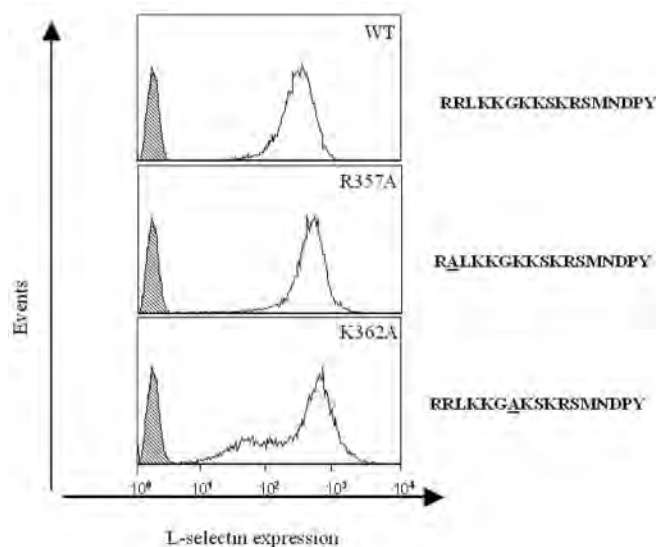


**FIG. 2. Generation of cell lines expressing WT and mutant forms of L-selectin.** Flow cytometric analysis of 300.19 cell lines expressing WT, R357A, and K362A L-selectin, stained with FITC-conjugated anti-L-selectin antibody. The FACS profile of puromycin-resistant, L-selectin-negative, 300.19 cells is positioned to the left in every FACS plot (gray). L-selectin tail sequences are listed to the right of every FACS plot, and *underlined* alanine residues denote the position of mutation.

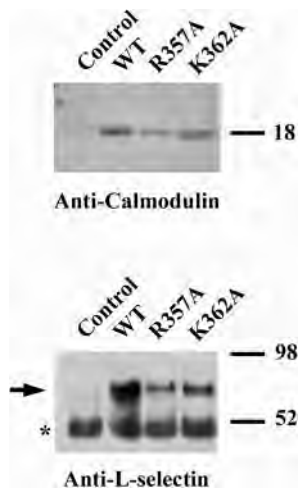


**FIG. 3. Calmodulin co-precipitates with WT, R357A and K362A L-selectin.** Antiserum JK942 was used to immunoprecipitate L-selectin from WT, R357A, and K362A cell lines. Immunoprecipitates were resolved on SDS-PAGE and transferred to nitrocellulose filters. Anti-calmodulin antibodies were used to detect calmodulin (upper panel). Immunoblot of immunoprecipitate was subsequently probed with anti-L-selectin monoclonal antibody, CA21 (lower panel), to detect relative levels of L-selectin that had been immunoprecipitated. The black arrowhead indicates the position of L-selectin. The asterisk indicates the position of heavy chain immunoglobulin (lower panel).

leukocytes (40, 41). Using transmission electron microscopy, we compared the localization of R357A or K362A L-selectin with WT selectin (Fig. 5). Immunogold labeling of L-selectin demonstrated that WT L-selectin was predominantly positioned on microvilli (Fig. 5B). In contrast, R357A and K362A L-selectin were positioned predominantly on the cell body (~75 and 68%, respectively). Scanning electron microscopy showed no differences in microvillar morphology between 300.19 cells expressing WT, R357A, K362A, or control cells with no L-selectin (data not shown). These results suggest that interaction of the L-selectin tail with ERM proteins is important for microvillar positioning of L-selectin.

**L-selectin-dependent Rolling on Saturating Levels of Ligand Is Unaffected by ERM-binding Mutations**—L-selectin-dependent rolling of leukocytes is sensitive to toxins that inhibit *de novo* polymerization of F-actin (14–16), and it is believed that attachment of L-selectin to the actin cytoskeleton is essential for rolling. In addition to  $\alpha$ -actinin, the ERM proteins could potentially link L-selectin with the actin cytoskeleton. Rolling assays were therefore performed using the 300.19 pre-B cell lines expressing WT, R357A, and K362A L-selectin. Rolling velocities were analyzed using a parallel plate flow chamber at a fixed shear stress of 2.5 dynes/cm<sup>2</sup>. Recombinant PSGL-1 fused to human immunoglobulin heavy chain (rPSGL-1-Ig) was used as a ligand in all rolling assays.

Rolling on rPSGL-1-Ig was found to be L-selectin-dependent, since control L-selectin-negative puromycin-resistant cells were unable to roll on rPSGL-1-Ig. Furthermore, L-selectin-positive cells did not roll in the absence of immobilized rPSGL-1-Ig (data not shown). Titration of rPSGL-1-Ig indicated that saturating levels of ligand were achieved at 63.4  $\mu$ g/ml, whereas at 6.34  $\mu$ g/ml, levels were submaximal (Fig. 6A). In support of this, cells expressing WT, R357A, and K362A L-selectin had similar rolling velocities on 63.4  $\mu$ g/ml and 634  $\mu$ g/ml rPSGL-1-Ig (data not shown), suggesting that a concentration of 63.4  $\mu$ g/ml is saturating.

The number of rolling events for each cell line did not vary significantly, and few adherent cells were observed when rPSGL-1-Ig was immobilized at a concentration of 63.4  $\mu$ g/ml (Fig. 6B). Similar mean rolling velocities were observed for all three cell lines, suggesting that mutagenesis of the ERM-binding domain of the L-selectin tail did not affect their relative velocities (Fig. 6C). The proportion of cells that were rolling (*i.e.* with velocities of <200  $\mu$ m/s) to cells that were free-flowing (*i.e.* with velocities of >200  $\mu$ m/s) was unchanged between WT and ERM-binding mutants (Fig. 6D).

It is possible that differences in the levels of L-selectin on the surface of K362A and R357A cell lines compared with WT cells could affect their rolling behavior, masking effects of the ERM-binding mutations on rolling. In order to exclude this possibility, single-cell clones were generated from cells expressing R357A L-selectin, which expressed L-selectin levels that matched WT and K362A L-selectin, which had more homogeneous levels than before (compare profiles of Fig. 2A with profiles of Fig. 7A). Both clones had rolling velocities on rPSGL-1-Ig similar to the values shown in Fig. 6 (data not shown), indicating that the range of L-selectin expression levels used here do not significantly affect rolling velocity.

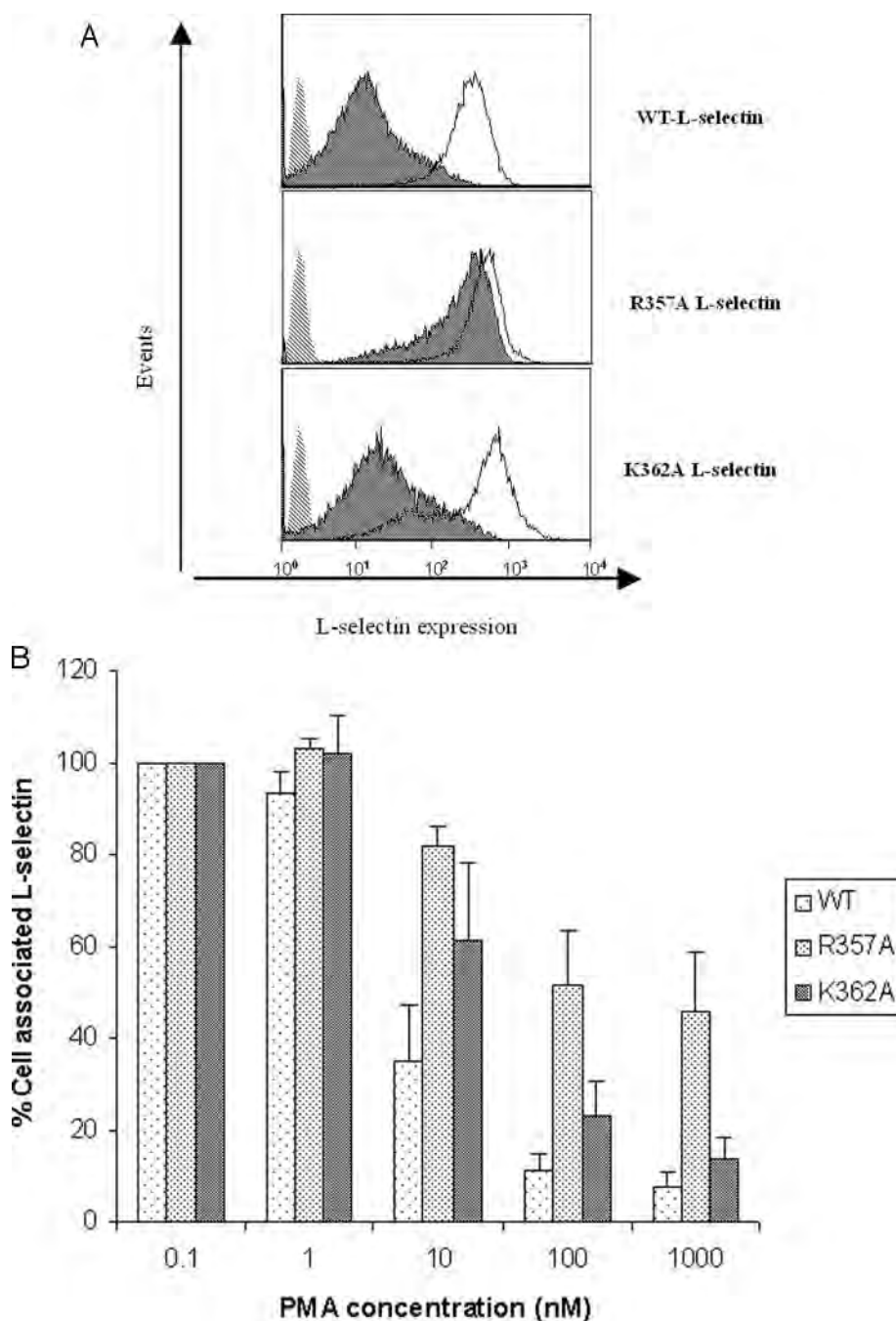
**Cells Expressing ERM-binding Mutants of L-selectin Have Reduced Tethering Efficiency**—Subsaturating levels of immobilized rPSGL-1-Ig resulted in fewer rolling events (Fig. 7B) but still allowed tethering events to occur (Fig. 7C). Under these conditions, cells expressing WT, R357A, and K362A could be monitored for their ability to tether. We found that tethering efficiencies in cells expressing R357A and K362A L-selectin were reduced by ~50% when compared with WT L-selectin (Fig. 7C). These results indicate that ERM/L-selectin interaction is involved in leukocyte tethering.

## DISCUSSION

Here we report for the first time the relevance of ERM/L-selectin tail interaction in cells. We demonstrate that L-selectin mutants defective in moesin binding have reduced localization to microvilli, impaired tethering, and PMA-induced shedding (Fig. 8).

With the exception of tethering, we have observed consistent differences in the severity of the phenotypes between the two moesin-binding mutants. Cells expressing R357A have less L-selectin on microvilli and lower PMA-induced shedding than

**FIG. 4. Comparison of PMA-induced shedding between cells expressing WT, R357A, and K362A L-selectin.** *A*, FACS plot overlays of cells treated with (unshaded profile) or without (shaded profile) 1  $\mu$ M PMA. Each cell line was stimulated for 15 min at 37 °C. Cells were subsequently labeled with FITC-conjugated anti-L-selectin antibody. Light gray-shaded FACS profiles indicate position of puromycin-resistant, L-selectin-negative cells. *B*, dose response of PMA stimulation with respect to L-selectin shedding. 300.19 cells, stably expressing WT, R357A, and K362A stable transfectants were incubated with 0.1, 1, 10, 100, or 1000 nM PMA for 15 min at 37 °C. The percentage of cell-associated L-selectin was calculated as the difference in mean fluorescence intensity between PMA-stimulated cells and mock-stimulated cells for each cell line. Results are expressed as the mean  $\pm$  S.D. of three independent experiments.



cells expressing K362A. Neither the R357A nor the K362A peptide interacts detectably with N-terminal moesin *in vitro*, and thus they are both defective in moesin binding, but it is possible that their relative affinities for moesin differ or that they have differential abilities to bind to moesin in cells. Structural analysis of the L-selectin tail bound to moesin should reveal how these amino acids contribute to the interaction.

We find that PMA-induced shedding of L-selectin is affected in cells expressing both R357A and K362A L-selectin. Since both mutants are predominantly excluded from microvilli, it is possible that these mutants are segregated from the enzyme, ADAM17, which could account for their resistance to PMA-induced shedding. Indeed, ADAM17 has been reported to have a punctate domain distribution on the plasma membrane of monocytes (42), which could be microvilli. An alternative explanation is that interaction between L-selectin tail and ERM proteins promotes association with ADAM17 and shedding of L-selectin.

Indeed, we have previously shown that stimulation of primary lymphocytes with PMA induces the association of moesin, but not ezrin, with L-selectin tail (17), indicating that the interaction of L-selectin with moesin is regulated and could coincide with PMA-induced shedding. A previous report using CD44/L-selectin and CD31/L-selectin chimerae also suggests that L-selectin shedding is not restricted to microvilli (38). These chimerae possess the cytoplasmic and transmembrane domains of either CD31 or CD44 fused to the extracellular domain of L-selectin and are respectively randomly distributed on the plasma membrane or excluded from microvilli. However, both chimerae can undergo rapid PMA-induced shedding as efficiently as WT L-selectin, suggesting that ADAM17 activity is not restricted to microvilli. Since both CD44 and CD31 have been reported to interact with ERM proteins (30, 43), mutagenesis of the ERM-binding domains within the cytoplasmic tails of CD31/L-selectin and CD44/L-selectin chimerae may reveal whether ERM proteins play a direct

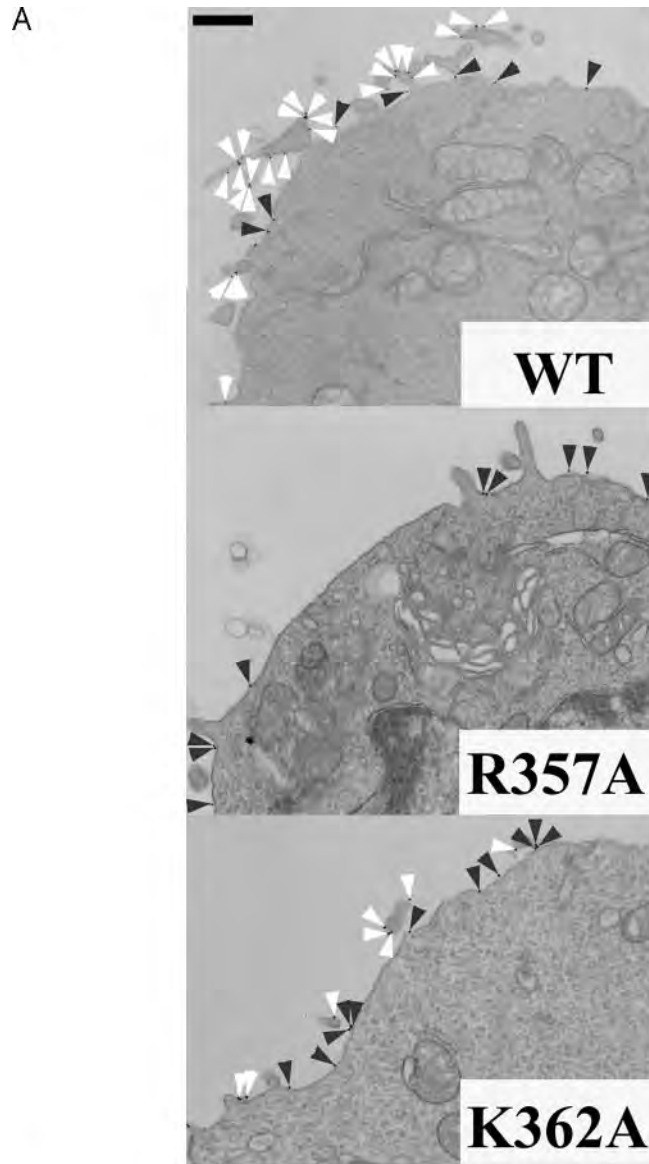
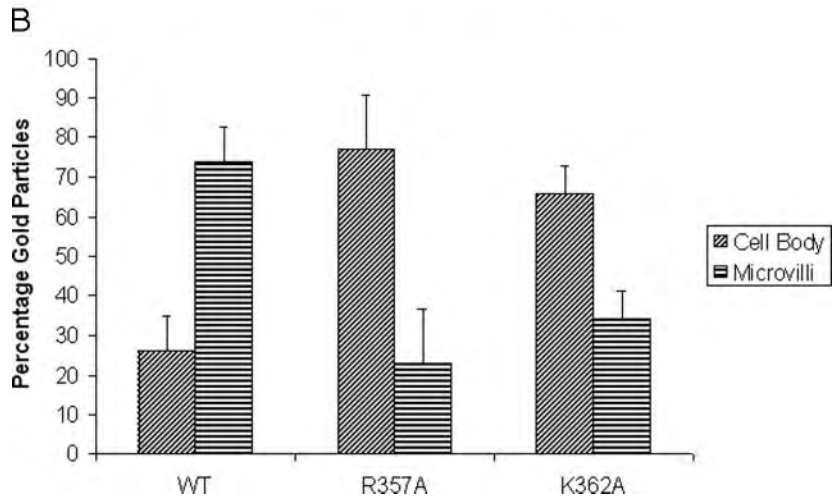


**FIG. 5. Microvillar localization of WT and ERM-binding mutants of L-selectin.** *A*, transmission electron micrographs of 300.19 pre-B cells stably expressing WT, R357A, and K362A L-selectin. Labeling of cells was performed as described under “Experimental Procedures.” The *white arrowheads* indicate gold particle labeling of L-selectin positioned on microvillar structures. The *black arrowheads* indicate gold particle labeling not on microvillar structures. *Bar*, 500 nm. *B*, results of counting gold particles resident on either the cell body or microvilli of stable transfectants expressed as a percentage (see “Experimental Procedures”). Results are represented as the mean  $\pm$  S.D. of three independent experiments. Approximately 35 cells were counted in each experiment, and 1000–1500 gold particles were counted for each experiment.



or indirect role in PMA-induced shedding. Although we do not observe a decrease in R357A and K362A L-selectin association with calmodulin in cells, it is possible that they bind more tightly to calmodulin and that this contributes to their resistance to PMA-induced shedding.

It is noteworthy that CD44 is not localized to microvilli in leukocytes (44), although it is in other cell types (43). This suggests that other proteins apart from ERM proteins may contribute to microvillar positioning of CD44. It is possible that  $\alpha$ -actinin also contributes to L-selectin localization, and thus

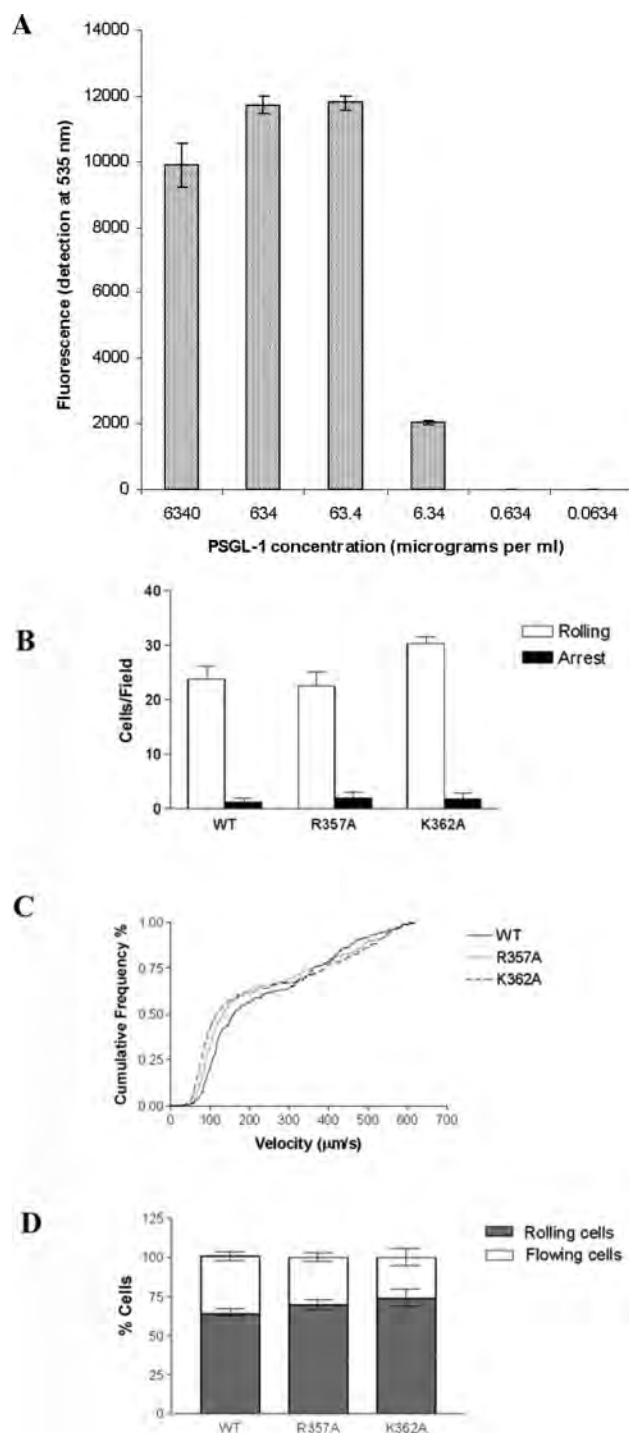


**FIG. 6. Mutagenesis of the ERM-binding domain of L-selectin tail does not affect rolling behavior on immobilized rPSGL-1-Ig.** **A**, detection of rPSGL-1-Ig immobilized on plastic microtiter wells (Nunc). rPSGL-1-Ig was detected using FITC-conjugated anti-human PSGL-1 (mouse monoclonal KPL1 antibody) as described under "Experimental Procedures." Results are expressed as the mean  $\pm$  S.D. of three independent experiments. In each rolling experiment, cells were perfused at a density of  $3 \times 10^5/\text{ml}$  at  $37^\circ\text{C}$  over slides (Nunc) coated with  $63.4 \mu\text{g}/\text{ml}$  rPSGL-1-Ig. **B**, comparative analysis of rolling and arrested 300.19 cells expressing WT, R357A, or K362A L-selectin. Data were collected and expressed as the mean  $\pm$  S.D. of three independent rolling experiments. Puromycin-resistant, L-selectin-negative 300.19 cells were unable to roll on immobilized rPSGL-1-Ig (data not shown). **C**, at least 300 individual cells were tracked for a period of 5 min. The mean velocity of each individual cell was recorded (see "Experimental Procedures") and expressed as percentage of cumulative frequency. **D**, relative percentages of free-flowing ( $>200 \mu\text{m}/\text{s}$ ) and rolling ( $<200 \mu\text{m}/\text{s}$ ) cells analyzed in **C** expressed as the mean  $\pm$  S.D. from three independent experiments.

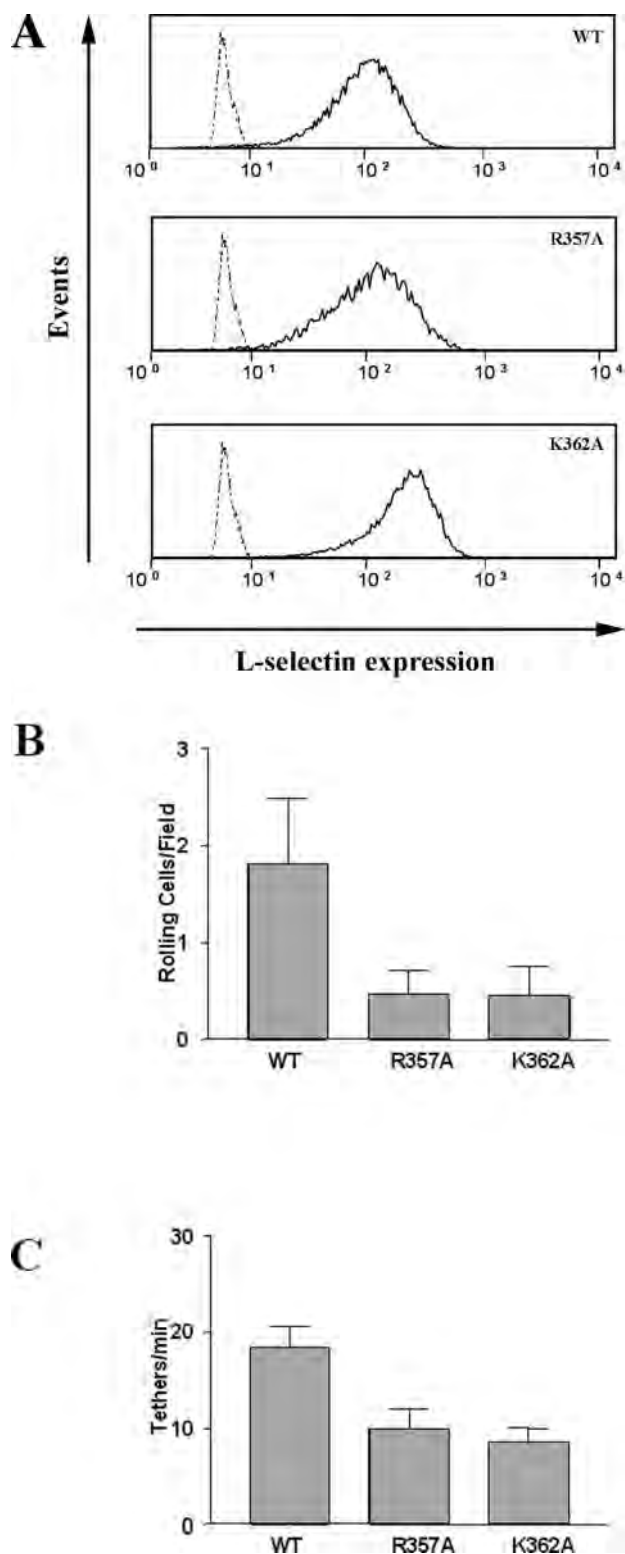


**FIG. 7. Tethering efficiency is reduced in cells expressing R357A and K362A L-selectin.** **A**, FACS plots showing L-selectin levels on 300.19 cells expressing WT, R357A, and K362A L-selectin. The cells expressing R357A and K362A L-selectin were derived from single cell clones. The cell line expressing WT L-selectin is the same as that shown in Fig. 2A. The FACS profile of L-selectin-negative puromycin-resistant 300.19 cells is positioned at the left in each FACS plot. **B**, number of cells rolling on slides coated with subsaturating ( $31.7 \mu\text{g}/\text{ml}$ ) amounts of rPSGL-1-Ig. **C**, the number of functional tethers are expressed as the number of tethering events/min (see "Experimental Procedures"). All tethering experiments were performed at a fixed shear stress of  $2.5 \text{ dynes}/\text{cm}^2$ . The cell lines used in **B** and **C** are the same as those shown in **A**. Results in **B** and **C** are expressed as the mean  $\pm$  S.D. of three independent experiments.

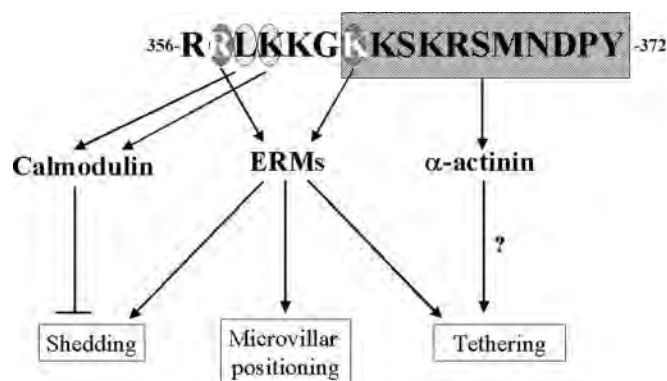


**FIG. 8. Schematic diagram of L-selectin tail and its binding partners.** Residues on L-selectin tail that are necessary for interaction with calmodulin and ERM proteins are indicated within *oval shaded areas*. Oblong shading defines the  $\alpha$ -actinin binding domain. The ERM protein binding site either overlaps or is juxtaposed to the  $\alpha$ -actinin and calmodulin binding sites, respectively. ERM proteins could therefore have roles that are either overlapping or antagonistic to both  $\alpha$ -actinin and calmodulin. Our results indicate that ERM proteins are required for microvillar positioning, leukocyte tethering, and L-selectin shedding. The  $\alpha$ -actinin-binding domain is intact in cells expressing R357A L-selectin, which suggests that  $\alpha$ -actinin is not sufficient for tethering. Moesin is recruited to L-selectin tail upon PMA stimulation and could facilitate shedding of L-selectin by inducing a conformational change in the cleavage site that renders it susceptible to proteolysis.

defining residues within L-selectin tail that interact with  $\alpha$ -actinin will be important for determining the role of the  $\alpha$ -actinin/L-selectin interaction (Fig. 8).

Our results suggest a possible model where calmodulin and ERM proteins act antagonistically to regulate L-selectin shedding (Fig. 8). Release of calmodulin from the L-selectin tail could allow ERM proteins to bind and stabilize a conformation that makes the ectodomain of L-selectin susceptible to proteolysis.

The necessity for microvillar positioning of L-selectin during leukocyte tethering has been well documented (45, 46). We have observed that, when compared with WT L-selectin, the ERM-binding mutants R357A and K362A L-selectin have reduced tethering efficiencies on PSGL-1 and decreased localization to microvilli, consistent with a model where ERM proteins target L-selectin to microvilli.

In contrast to their effects on tethering, rolling velocities do not vary between ERM-binding mutants and WT L-selectin under saturating ligand conditions. This is in line with previous observations that microvillar exclusion of L-selectin does not affect leukocyte rolling (45) but does affect tethering efficiency (46). The first 6 amino acids of the L-selectin tail (L $\Delta$ cyto, which does not include Lys<sup>362</sup>; see Fig. 8) can support L-selectin-dependent rolling of 300.19 cells, although less efficiently than cells expressing WT L-selectin (16). Furthermore, the rolling velocities of lymphocytes expressing WT CD44 or an ERM-binding mutant of CD44 are similar (44). It is possible that L-selectin/ERM protein interaction contributes to rolling under other conditions (*e.g.* on subsaturating concentrations of rPSGL-1Ig or on other ligands), and this will be important to test in the future.

Many reports have described L-selectin as a signaling receptor (47–54). The mechanism by which L-selectin transduces signals is currently not known. Moesin has been recently implicated as a signaling adaptor molecule for PSGL-1-mediated signaling (55). Determining whether ERM proteins have a role in L-selectin-mediated signal transduction will be an important focus for future research.

**Acknowledgments**—We thank Arnold Pizzey (Department of Hematology, University College, London) for invaluable help with cell sorting and FACS analysis and Geoffrey Kansas for advice on rolling experi-

ments. We are grateful to Thomas Tedder, Julius Kahn, and David Sacks for pMT2/LAM plasmid containing L-selectin cDNA, 300.19 pre-B-cells, JK942 anti-L-selectin serum, and anti-calmodulin monoclonal antibodies, respectively. We also thank Wyeth Research (Cambridge MA) for rPSGL-Ig protein for rolling and tethering experiments.

## REFERENCES

- Springer, T. A. (1994) *Cell* **76**, 301–314
- Arbones, M. L., Ord, D. C., Ley, K., Ratech, H., Maynard-Curry, C., Otten, G., Capon, D. J., and Tedder, T. F. (1994) *Immunity* **1**, 247–260
- Khan, A. I., Landis, R. C., and Malhotra, R. (2003) *Inflammation* **27**, 265–280
- Kishimoto, T. K., Jutila, M. A., Berg, E. L., and Butcher, E. C. (1989) *Science* **245**, 1238–1241
- Alexander, S. R., Kishimoto, T. K., and Walcheck, B. (2000) *J. Leukocyte Biol.* **67**, 415–422
- Kahn, J., Ingraham, R. H., Shirley, F., Migaki, G. I., and Kishimoto, T. K. (1994) *J. Cell Biol.* **125**, 461–470
- Zhao, L., Shey, M., Farnsworth, M., and Dailey, M. O. (2001) *J. Biol. Chem.* **276**, 30631–30640
- Peschon, J. J., Slack, J. L., Reddy, P., Stocking, K. L., Sunnarborg, S. W., Lee, D. C., Russell, W. E., Castner, B. J., Johnson, R. S., Fitzner, J. N., Boyce, R. W., Nelson, N., Kozlosky, C. J., Wolfson, M. F., Rauch, C. T., Cerretti, D. P., Paxton, R. J., March, C. J., and Black, R. A. (1998) *Science* **282**, 1281–1284
- Condon, T. P., Flournoy, S., Sawyer, G. J., Baker, B. F., Kishimoto, T. K., and Bennett, C. F. (2001) *Antisense Nucleic Acid Drug Dev.* **11**, 107–116
- Gomez-Gavero, M. V., Gonzalez-Alvaro, I., Dominguez-Jimenez, C., Peschon, J., Black, R. A., Sanchez-Madrid, F., and Diaz-Gonzalez, F. (2002) *J. Biol. Chem.* **277**, 38212–38221
- Kahn, J., Walcheck, B., Migaki, G. I., Jutila, M. A., and Kishimoto, T. K. (1998) *Cell* **92**, 809–818
- Matala, E., Alexander, S. R., Kishimoto, T. K., and Walcheck, B. (2001) *J. Immunol.* **167**, 1617–1623
- Diaz-Rodriguez, E., Esparis-Ogando, A., Montero, J. C., Yuste, L., and Pandiella, A. (2000) *Biochem. J.* **346**, 359–367
- Pavalko, F. M., Walker, D. M., Graham, L., Goheen, M., Doerschuk, C. M., and Kansas, G. S. (1995) *J. Cell Biol.* **129**, 1155–1164
- Kansas, G. S., Ley, K., Munro, J. M., and Tedder, T. F. (1993) *J. Exp. Med.* **177**, 833–838
- Dwir, O., Kansas, G. S., and Alon, R. (2001) *J. Cell Biol.* **155**, 145–156
- Ivetić, A., Deka, J., Ridley, A., and Ager, A. (2002) *J. Biol. Chem.* **277**, 2321–2329
- Ivetić, A., and Ridley, A. J. (2004) *Immunology* **112**, 165–176
- Amieva, M. R., and Furthmayr, H. (1995) *Exp. Cell Res.* **219**, 180–196
- Yonemura, S., Nagafuchi, A., Sato, N., and Tsukita, S. (1993) *J. Cell Biol.* **120**, 437–449
- Tsukita, S., and Yonemura, S. (1999) *J. Biol. Chem.* **274**, 34507–34510
- Tsukita, S., Oishi, K., Sato, N., Sagara, J., and Kawai, A. (1994) *J. Cell Biol.* **126**, 391–401
- Barreiro, O., Yanez-Mo, M., Serrador, J. M., Montoya, M. C., Vicente-Manzanares, M., Tejedor, R., Furthmayr, H., and Sanchez-Madrid, F. (2002) *J. Cell Biol.* **157**, 1233–1245
- Serrador, J. M., Alonso-Lebrero, J. L., del Pozo, M. A., Furthmayr, H., Schwartz-Albiez, R., Calvo, J., Lozano, F., and Sanchez-Madrid, F. (1997) *J. Cell Biol.* **138**, 1409–1423
- Yonemura, S., Hirao, M., Doi, Y., Takahashi, N., Kondo, T., and Tsukita, S. (1998) *J. Cell Biol.* **140**, 885–895
- Serrador, J. M., Vicente-Manzanares, M., Calvo, J., Barreiro, O., Montoya, M. C., Schwartz-Albiez, R., Furthmayr, H., Lozano, F., and Sanchez-Madrid, F. (2002) *J. Biol. Chem.* **277**, 10400–10409
- Serrador, J. M., Nieto, M., Alonso-Lebrero, J. L., del Pozo, M. A., Calvo, J., Furthmayr, H., Schwartz-Albiez, R., Lozano, F., Gonzalez-Amaro, R., Sanchez-Mateos, P., and Sanchez-Madrid, F. (1998) *Blood* **91**, 4632–4644
- Snapp, K. R., Ding, H., Atkins, K., Warnke, R., Luscinskas, F. W., and Kansas, G. S. (1998) *Blood* **91**, 154–164
- Serrador, J. M., Urzainqui, A., Alonso-Lebrero, J. L., Cabrero, J. R., Montoya, M. C., Vicente-Manzanares, M., Yanez-Mo, M., and Sanchez-Madrid, F. (2002) *Eur. J. Immunol.* **32**, 1560–1566
- Gamulescu, M. A., Seifert, K., Tingart, M., Falet, H., and Hoffmeister, K. M. (2003) *Platelets* **14**, 211–217
- Pearson, M. A., Reczek, D., Bretscher, A., and Karplus, P. A. (2000) *Cell* **101**, 259–270
- Szabo, A., Stolz, L., and Granzow, R. (1995) *Curr. Opin. Struct. Biol.* **5**, 699–705
- Ley, K., Tedder, T. F., and Kansas, G. S. (1993) *Blood* **82**, 1632–1638
- Zakrzewicz, A., Grafe, M., Terbeek, D., Bongrazio, M., Auch-Schwell, W., Walzog, B., Graf, K., Fleck, E., Ley, K., and Gaehtgens, P. (1997) *Blood* **89**, 3228–3235
- Lawrence, M. B., Kansas, G. S., Kunkel, E. J., and Ley, K. (1997) *J. Cell Biol.* **136**, 717–727
- Preece, G., Murphy, G., and Ager, A. (1996) *J. Biol. Chem.* **271**, 11634–11640
- Borland, G., Murphy, G., and Ager, A. (1999) *J. Biol. Chem.* **274**, 2810–2815
- Fors, B. P., Goodarzi, K., and von Andrian, U. H. (2001) *J. Immunol.* **167**, 3642–3651
- Zhao, L. C., Edgar, J. B., and Dailey, M. O. (2001) *Dev. Immunol.* **8**, 267–277
- Erlandsen, S. L., Hasslen, S. R., and Nelson, R. D. (1993) *J. Histochem. Cytochem.* **41**, 327–333
- Borregaard, N., Kjeldsen, L., Sengelov, H., Diamond, M. S., Springer, T. A., Anderson, H. C., Kishimoto, T. K., and Bainton, D. F. (1994) *J. Leukocyte*

- Biol.* **56**, 80–87
42. Doedens, J. R., and Black, R. A. (2000) *J. Biol. Chem.* **275**, 14598–14607
43. Legg, J. W., and Isacke, C. M. (1998) *Curr. Biol.* **8**, 705–708
44. Gal, I., Lesley, J., Ko, W., Gonda, A., Stoop, R., Hyman, R., and Mikecz, K. (2003) *J. Biol. Chem.* **278**, 11150–11158
45. von Andrian, U. H., Hasslen, S. R., Nelson, R. D., Erlandsen, S. L., and Butcher, E. C. (1995) *Cell* **82**, 989–999
46. Stein, J. V., Cheng, G., Stockton, B. M., Fors, B. P., Butcher, E. C., and von Andrian, U. H. (1999) *J. Exp. Med.* **189**, 37–50
47. Brenner, B., Gulbins, E., Busch, G. L., Koppenhoefer, U., Lang, F., and Linderkamp, O. (1997) *Biochem. Biophys. Res. Commun.* **231**, 802–807
48. Brenner, B., Gulbins, E., Schlottmann, K., Koppenhoefer, U., Busch, G. L., Walzog, B., Steinhausen, M., Coggeshall, K. M., Linderkamp, O., and Lang, F. (1996) *Proc. Natl. Acad. Sci. U. S. A.* **93**, 15376–15381
49. Brenner, B., Grassme, H. U., Muller, C., Lang, F., Speer, C. P., and Gulbins, E. (1998) *Exp. Cell Res.* **243**, 123–128
50. Brenner, B., Weinmann, S., Grassme, H., Lang, F., Linderkamp, O., and Gulbins, E. (1997) *Immunology* **92**, 214–219
51. Malhotra, R., Priest, R., and Bird, M. I. (1996) *Biochem. J.* **320**, 589–593
52. Malhotra, R., and Bird, M. I. (1997) *Chem. Biol.* **4**, 543–547
53. Malhotra, R., and Bird, M. I. (1997) *BioEssays* **19**, 919–923
54. Turutin, D. V., Kubareva, E. A., Pushkareva, M. A., Ullrich, V., and Sud'ina, G. F. (2003) *FEBS Lett.* **536**, 241–245
55. Urzainqui, A., Serrador, J. M., Viedma, F., Yanez-Mo, M., Rodriguez, A., Corbi, A. L., Alonso-Lebrero, J. L., Luque, A., Deckert, M., Vazquez, J., and Sanchez-Madrid, F. (2002) *Immunity* **17**, 401–412

---

**Molecular Basis of Cell and  
Developmental Biology:  
Mutagenesis of the Ezrin-Radixin-Moesin  
Binding Domain of L-selectin Tail Affects  
Shedding, Microvillar Positioning, and  
Leukocyte Tethering**

Aleksandar Ivetic, Oliver Florey, Jürgen  
Deka, Dorian O. Haskard, Ann Ager and  
Anne J. Ridley

*J. Biol. Chem.* 2004, 279:33263-33272.

doi: 10.1074/jbc.M312212200 originally published online June 3, 2004

---

Access the most updated version of this article at doi: [10.1074/jbc.M312212200](https://doi.org/10.1074/jbc.M312212200)

Find articles, minireviews, Reflections and Classics on similar topics on the [JBC Affinity Sites](https://www.jbc.org/).

Alerts:

- [When this article is cited](#)
- [When a correction for this article is posted](#)

[Click here](#) to choose from all of JBC's e-mail alerts

This article cites 53 references, 32 of which can be accessed free at  
<http://www.jbc.org/content/279/32/33263.full.html#ref-list-1>